# Autoxidation of terpenes, a common pathway in tropospheric and low temperature combustion conditions: the case of limonene and α-pinene.

Roland Benoit [1] Nesrine Belhadj[1,2], Maxence Lailliau[1,2], and Philippe Dagaut[1]

[1]CNRS-INSIS, ICARE, Orléans, France, roland.benoit@cnrs-orleans.fr, nesrine.belhadj@cnrs-orleans.fr, maxence.lailliau@cnrs-orleans.fr, dagaut@cnrs-orleans.fr
[2]Université d'Orléans, Orléans, France

**Correspondence**: Roland Benoit (roland.benoit@cnrs-orleans.fr)

**Abstract.**

The oxidation of monoterpenes under atmospheric conditions has been the subject of numerous studies. They were motivated by the formation of oxidized organic molecules (OOM) which, due to their low vapor pressure, contribute to the formation of secondary organic aerosols (SOA). Among the different reaction mechanisms proposed for the formation of these oxidized chemical compounds, it appears that the autoxidation mechanism, common to both low-temperature combustion and atmospheric conditions, is important. We used the present combustion data and literature data from tropospheric oxidation studies to investigate possible similarities in terms of observed chemical formulae of OOM. Two terpenes, α-pinene and limonene, among the most abundant biogenic components in the atmosphere were considered. We built an experimental database consisting of literature atmospheric oxidation data and presently obtained combustion data. In order to probe the effects of the type of ionization used in mass spectrometry analyses on the detection of OOM, we used heated electrospray ionization (HESI) and atmospheric pressure chemical ionization (APCI), in positive and negative modes. The oxidation of limonene-oxygen-nitrogen and α-pinene-oxygen-nitrogen mixtures was performed using a jet-stirred reactor at elevated temperature (590 K), a residence time of 2 s, and atmospheric pressure. Samples of the reacting mixtures were collected in acetonitrile and analyzed by high-resolution mass spectrometry (Orbitrap Q-Exactive) after direct injection and soft ionization. This work shows a surprisingly similar set of chemical formulae of OOM and oligomers, formed in cool flames and under simulated atmospheric conditions. Data analysis showed that a non-negligible subset of chemical formulae is common to all experiments, independently of experimental parameters. Finally, this study indicates that more than 40% of the detected chemical formulae in this full dataset can be ascribed to an autoxidation mechanism.

## 1 Introduction

The links between atmospheric and combustion chemistry have often been studied from the point of view of tropospheric reactions of combustion effluents or pollutants, e.g., oxidation of volatile organic compounds, nitrogen oxides reactions, sulfur chemistry (Barsanti et al., 2017;Shrivastava et al., 2017;Zhao et al., 2018;Bianchi et al., 2019). Climate change and the increase of large wildfire events have profoundly modified the relationship between atmospheric chemistry and combustion at large. Among the factors contributing to climate change,

biomass burning is an important source of gases and aerosols in the atmosphere on a regional and global scale. These contributions, estimated at more than 90% for primary aerosols at the global level, have an impact on the chemical composition of the atmosphere (Chen et al., 2017;Andreae, 2019;Fawaz et al., 2021). Furthermore, Van Krevelen analyses of biomass burning samples indicated the presence of HOMs with O/C > 0.6 (Smith et al., 2009). When studying the oxidation of chemicals and the formation of SOA in the atmosphere, it becomes necessary to determine the contribution of different oxidation pathways pertaining to atmospheric chemistry, combustion chemistry, or both.

In low-temperature combustion (cool flame) the formation of oxidized organic molecules (OOM) is mainly attributed to autoxidation reactions (Affleck and Fish, 1967;Fish, 1968;Belhadj et al., 2021;Benoit et al., 2021) , whereas in atmospheric chemistry, it is only relatively recently that this pathway has been considered (Vereecken et al., 2007;Crounse et al., 2013;Jokinen et al., 2014a;Berndt et al., 2015;Jokinen et al., 2015b;Berndt et al., 2016;Iyer et al., 2021). Also, it has been identified that highly oxygenated molecules (HOMs), a source of secondary organic aerosols (SOA), can result from autoxidation processes (Wang et al., 2021b;Tomaz et al., 2021;Bianchi et al., 2019). Modeling studies complemented by laboratory experiments showed that autoxidation mechanisms proceed simultaneously on different peroxy radicals ($RO_2^{\cdot}$ stands for peroxy radicals) leading to, through isomerization and addition of $O_2$, the production of a wide range of oxidized compounds in a few hundred of a seconds (Jokinen et al., 2014a;Berndt et al., 2016;Bianchi et al., 2019). Autoxidation is based on an H-shift and oxygen addition which starts with the initial production of $RO_2^{\cdot}$. This mechanism can repeat itself several times, yielding HOMs. It can be competitive under atmospheric conditions, in pristine environments, with other reaction pathways involving $RO_2^{\cdot}$ (Bianchi et al., 2019;Vereecken and Nozière, 2020). Scheme 1 presents the autoxidation mechanism and complementary reaction pathways.

**Scheme 1. Autoxidation mechanism and complementary reaction pathways**

| Autoxidation pathways involving $RO_2^{\bullet}$ |
|---|
| $R^{\bullet} \xrightarrow{+O_2} ROO^{\bullet} \xrightarrow{\text{H-shift}} {}^{\bullet}QOOH \xrightarrow{+O_2} {}^{\bullet}OOQOOH \xrightarrow{\text{H-shift}} HOOQ^{\bullet}OOH \xrightarrow{+O_2} (HOO)_2Q^{\bullet}OO^{\bullet} \dashrightarrow$ <br> *(1) first $O_2$-addition* *(2) second $O_2$-addition* *(3) third $O_2$-addition* |
| Other reaction pathways involving $RO_2^{\cdot}$ |
| Carbonyl channel: $ROO^{\bullet} \rightarrow R_{-H}O + OH$ |
| Hydroperoxide channel: $ROO^{\bullet} + HOO^{\bullet} \rightarrow ROOH + O_2$ and $RO^{\bullet} + {}^{\bullet}OH + O_2$ |
| Disproportionation reactions: $ROO^{\bullet} + R'OO^{\bullet} \rightarrow RO^{\bullet} + R'O^{\bullet} + O_2$ and $R_{-H}O + R'OH + O_2$ |
| Accretion reactions: $ROO^{\bullet} + R'OO^{\bullet} \rightarrow ROOR' + O_2$ |

A study published in 2021 showed that the oxidation of alkanes follows this autoxidation mechanism under both atmospheric and combustion conditions (Wang et al., 2021b). Also, that work confirmed that internal H-shifts in autoxidation can be promoted by the presence of functional groups, as predicted earlier (Otkjær et al., 2018) for $RO_2^{\cdot}$ containing OOH, OH, $OCH_3$, $CH_3$, C=O, or C=C groups. To further assess the importance of these pathways, available data must be compared along with their experimental specificities. In laboratory studies under simulated atmospheric conditions, oxidation occurs at near-ambient temperatures (250-300 K), at atmospheric pressure, in the presence of ozone and/or $OH^{\cdot}$ radicals ($OH^{\cdot}$ stands for hydroxyl radicals), and with low initial terpene

concentrations (5-50 ppm). In combustion, $OH^{\cdot}$, temperature, and pressure are driving autoxidation. Initial reactant concentrations are generally higher compared to atmospheric conditions, so as to compensate for the absence of ozone and/or $OH^{\cdot}$ as reactant, and get oxidation to proceed, since terpenes, as other hydrocarbons, react very slowly with $O_2$. Rising temperature increases isomerization rates and favors autoxidation, at the expense of other possible reactions of $RO_2^{\cdot}$ (Wang et al., 2021a). In atmospheric chemistry, at near room temperature, autoxidation can be initiated via two reaction mechanisms: reactions with ozone or with the $OH^{\cdot}$. Suppression of one of these pathways by scavengers generally changes the amount of chemical compound formed (sometimes a drastic decrease >90% was observed e.g. (Kenseth et al., 2018;Meusinger et al., 2017;Pospisilova et al., 2020), but does not affect the diversity of observed chemical formulae (Zhao et al., 2018;Pospisilova et al., 2020). It has been reported earlier that a temperature rise from 250 to 273K does not affect the distribution of HOMs (Quéléver et al., 2019) whereas Trostl et al. suggested that the distribution of HOMs is affected by temperature, α-pinene or particle concentration (Tröstl et al., 2016). Similarly, the experiments of Huang et al. (Huang et al., 2018) performed at different temperatures (223 K and 296 K) and precursor concentration (0.714 and 2.2 ppm of α-pinene) suggested that the physicochemical properties, such as the composition of the oligomers, can be affected by a variation of temperature. Both in combustion and atmospheric chemistry, autoxidation of carbon skeleton mainly with more than 10 carbon atoms can yield highly oxygenated molecules (HOMs), e.g., compounds containing more than 7 oxygen atoms (Benoit et al., 2021;Bianchi et al., 2019). The term 'HOM' is generally associated with atmospheric chemistry (Bianchi et al., 2019), but this nomenclature does not specify the chemical properties of a compound. In other words, in combustion we can also observe highly oxidized chemical compounds similar to those relevant to atmospheric chemistry. The broad range of chemical molecules formed and the impact of the experimental conditions on their character remain a subject for atmospheric chemistry and combustion chemistry studies. Moreover, whatever the mechanism of aerosol formation, i.e., oligomerization, addition, or accretion, their composition will be linked to that of the initial radicals pool (Tomaz et al., 2021).

In low-temperature combustion, when the temperature is increased, autoxidation rate goes through a maximum between 500 and 670 K, depending on the nature of the fuel (Belhadj et al., 2020;Belhadj et al., 2021), and the rate of formation of HOM also increases (Bianchi et al., 2019). Therefore, temperature has a measurable effect on the amount of HOMs formed (Wang et al., 2021b). In low-temperature combustion chemistry as in atmospheric chemistry, the oxidation of a chemical compound leads to the formation of several thousands of chemical compounds which result from successive additions of oxygen, isomerization, accretion, fragmentation, and oligomerization (Benoit et al., 2021). The exhaustive analysis of chemical compounds remains difficult, in the current state of instrumental limitations. This would consist in analyzing several thousands of molecules in $MS^2$ mode using separative techniques such as ultra-high pressure liquid chromatography (UHPLC) or ion mobility spectrometry (IMS) (Krechmer et al., 2016;Kristensen et al., 2016). Nevertheless, it is possible to classify these molecular compounds, considering only $C_xH_yO_z$ compounds, according to various criteria accessible via graphic tools representation such as van Krevelen diagrams, double bond equivalent number (DBE), and average carbon oxidation state (OSc) versus the number of carbon atoms (Kourtchev et al., 2015;Nozière et al., 2015). Such postprocessing of large datasets has the advantage of immediately highlighting families of compounds or physicochemical properties such as the condensation of molecules (vapor pressure), the large variety of oxygenated chemical compounds ($C_xH_yO_{1\text{-}15}$ in the present experiments) and the formation of oligomers (Kroll et al., 2011;Xie et al., 2020).

In addition to the recent studies focusing on the first steps of autoxidation, a more global approach, based on the comparison of possible chemical transformations related to autoxidation in low temperature combustion and atmospheric chemistry, is needed for evaluating the importance of autoxidation under tropospheric and low-temperature combustion conditions. In order to study the effects of ozonolysis and combustion on the diversity of chemical molecules formed by autoxidation, we have selected α-pinene (AP) and limonene (LM), two terpene isomers among the most abundant in the troposphere. These two monoterpenes with their distinctive characters are good candidates for studying autoxidation versus initial chemical structure and temperature. For AP, in addition to the reactivity of its endo-cyclic double bond, chemical compounds arising from ring opening of the cyclobutyl group have been detected, which could explain the diversity of observed oxidation chemical compounds as propose earlier (Kurtén et al., 2015;Iyer et al., 2021). This large pool of chemical compounds is increased in the case of LM by the presence of two double bonds (Hammes et al., 2019;Jokinen et al., 2015b). Nevertheless, the diversity of oxidation chemical compounds can be compensated by similarities in terms of reaction mechanisms and intermediates formed through autoxidation (Savee et al., 2015).

The present worked is a prolongation of that published earlier for the oxidation of LM alone (Benoit et al., 2021). We attempted to probe possible similitudes in terms of products' chemical formulae (product signals appearing with the same exact mass) observed under two different experimental conditions, i.e., (i) atmospheric oxidation and (ii) cool flame oxidation of terpenes and link them to common oxidation routes (Scheme 1). AP and LM were oxidized in a jet-stirred reactor at atmospheric pressure, excess of oxygen, and at a temperature of 590 K where the concentration of hydroperoxides and HOMs is maximal, under our experimental conditions. Then, we characterized the impact of using different ionization techniques (HESI and APCI) in positive and negative modes on the pool of detected chemical formulae. The particularities of each ionization mode were analyzed to identify the most suitable ionization technique for exploring the formation of autoxidation chemical compounds under low temperature combustion. Chemical formulae detected here and in atmospheric chemistry studies were compiled and tentatively used to evaluate the importance of autoxidation under both conditions.

## 2 Experiments

### 2.1 Oxidation experiments

The present experiments were carried out in a fused silica jet-stirred reactor (JSR) setup presented earlier (Dagaut et al., 1986;Dagaut et al., 1988) and used in previous studies (Dagaut et al., 1987;Benoit et al., 2021;Belhadj et al., 2021). AP and LM were studied separately, AP (+) (Sigma Aldrich, 98%) and LM (R)-(+) (Sigma-Aldrich,>97%), were pumped by an HPLC pump (Shimadzu LC10 AD VP) with an online degasser (Shimadzu DGU-20 A3) and sent to a vaporizer assembly where it was diluted by a nitrogen flow. Each terpene and oxygen, both diluted by $N_2$, were sent separately to a 42 mL JSR to avoid oxidation before reaching 4 injectors (nozzles of 1 mm I.D.) providing stirring. The flow rates of nitrogen and oxygen were controlled by mass flow meters. Good thermal homogeneity along the vertical axis of the JSR was recorded (gradients of < 1 K/cm) by thermocouple measurements (0.1 mm Pt-Pt/Rh-10% wires located inside a thin-wall silica tube) (Benoit et al., 2021;Belhadj et al., 2021). In order to observe the oxidation of these terpenes, which are not prone to strong self-ignition, the oxidation of 1% of these chemical compounds under lean fuel conditions (equivalence ratio 0.25, 56% $O_2$, 43% $N_2$), was carried out at 590 K, atmospheric pressure, and a residence time of 2 s. Under these conditions, the

oxidation of the two terpenes is initiated by slow H-atom abstraction by molecular oxygen. The experimental temperature was selected in order to be able to detect the formation of products of oxidation such as ketohydroperoxides and HOMs. Previous studies of ours showed a maximum formation of these chemical products at such a temperature (Belhadj et al., 2021). The fuel's radicals react rapidly with $O_2$ to form peroxy radicals which undergo further oxidation, characteristic of autoxidation. The absence of ozone, and no need for the addition of a scavenger, allow probing reaction mechanisms and observing chemical compounds potentially specific to autoxidation initiated by OH˙. A 2 mm I.D. probe was used to collect samples. To measure low-temperature oxidation chemical compounds ranging from early oxidation steps products to highly oxidized molecules, the sonic samples were bubbled in cooled acetonitrile (UHPLC grade ≥99.9%, T= 0°C, 250 mL) for 90 min. The resulting solution was stored in a freezer at -15°C. The stability of the chemical compounds collected in acetonitrile was verified and no detectable changes on a mass spectrum obtained on the orbitrap were observed after more than one month.

**2.2 Chemical analyses**

Analyses of samples collected in acetonitrile were performed by direct sample infusion (rate: 3µL/min and recorded for 1 min for data averaging) in the ionization chamber of a high-resolution mass spectrometer (Thermo Scientific Orbitrap® Q-Exactive, mass resolution 140,000 and mass accuracy <0.5 ppm RMS). Only qualitative measurements were performed here because of missing standards for calibration. Nevertheless, for products with the same exact mass, one can assume the signal increases with concentration. Both heated electrospray ionization (HESI) and atmospheric chemical ionization (APCI) were used in positive and negative modes. HESI settings were: spray voltage 3.8 kV, T vaporizer of 150°C, T capillary 200°C, sheath gas flow of 8 arbitrary units (a.u.), auxiliary gas flow of 1 a.u., sweep gas flow of 0 a.u.. In APCI, settings were: spray voltage 3.8 kV, vaporizer temperature of 150°C, capillary temperature of 200°C, sheath gas flow of 8 a.u., auxiliary gas flow of 1 a.u., sweep gas flow of 0 a.u., corona current of 3µA. In order to avoid transmission and detection effects of ions depending on their mass inside the C-Trap (Hecht et al., 2019), acquisitions with three mass ranges were performed (*m/z* 50-750; *m/z* 150-750; *m/z* 300-750). The upper limit of *m/z* 750 was chosen because of the absence of signal beyond this value. We verified that no significant oxidation occurred in the HESI and APCI ion sources by injecting a LM-ACN mixture. The optimization of the Orbitrap ionization parameters in HESI and APCI did not show any clustering phenomenon for these two terpenes. The parameters evaluated were: injection source, capillary distance, vaporization and capillary temperatures, applied difference of potential, injected volume, flow rate of nitrogen in the ionization source. Positive and negative HESI mass calibrations were performed using Pierce™ calibration mixtures (Thermo Scientific). Chemical compounds with relative intensity less than 1 ppm to the highest mass peak in the mass spectrum were not considered. Nevertheless, it should be considered that some of the chemical formulae reported in this study could result from our experimental conditions (continuous flow reactor, reagent concentration, temperature, reaction time) and to some extent from our acquisition conditions, different from those of the previous studies (Deng et al., 2021;Quéléver et al., 2019;Meusinger et al., 2017;Krechmer et al., 2016;Tomaz et al., 2021;Fang et al., 2017;Witkowski and Gierczak, 2017;Jokinen et al., 2015a;Nørgaard et al., 2013;Bateman et al., 2009;Walser et al., 2008;Warscheid and Hoffmann, 2001;Hammes et al., 2019;Kundu et al., 2012). Indeed, the use of a continuous flow reactor operating at elevated temperature, as well as a high initial

concentration of reagents can induce the formation of combustion-specific chemical compounds, which does not exclude their possible formation under atmospheric conditions.

## 3 Data Processing

High resolution mass spectrometry (HR-MS) generates a large amount of data that is difficult to fully analyze by sequential methods. When the study requires the processing of several thousands of molecules, the use of statistical tools and graphical representation means becomes necessary. In this study, we have chosen to use the van Krevelen diagram (Van Krevelen, 1950) by adding an additional dimension, the double bond equivalent (DBE). The DBE number represents the sum of unsaturation and rings present in a chemical compound (Melendez-Perez et al., 2016).

$$DBE = 1 + C - H/2 - O \quad (1)$$

This number is independent of the number of oxygen atoms, but changes with the number of hydrogen atoms. Decimal values of this number, which correspond to an odd number of hydrogen atoms, were not considered in this study. Then, duplications of chemical formulae in the O/C vs. H/C space are eliminated. The oxidation state of carbon (OSc) provides a measure of the degree of oxidation of chemical compounds (alcohols, aldehydes, carboxylic acids, esters, ethers and ketones, but not peroxides) (Kroll et al., 2011). This provides a framework for describing the chemistry of organic compounds. It is defined by the following equation:

$$OSc \approx 2\ O/C - H/C \quad (2)$$

## 4 Results and discussion

### 4.1 Characterization of ionization sources

According to the experimental conditions described in Section 2, we obtained a different number of ions depending on the ionization source and the polarity used. Table 1 shows the number of ions detected according to the experimental conditions.

**Table 1.** Number of ions detected for each source in positive and negative modes.

| Ionization source | α-Pinene | | Limonene | |
|---|---|---|---|---|
| APCI | 646 (+) | 503(-) | 1321(+) | 1346(-) |
| HESI | 594(+) | 693(-) | 1017(+) | 1864(-) |

The sets of chemical compounds obtained were compared (under their molecular form) thanks to Venn diagrams. These sets have common data, but also specific chemical formulae. For a given ionization source, less than 50% of the chemical formulae are common to both polarities. In other words, between 30 and 50% of molecular compounds are ignored when using a single polarity. It is therefore essential to use both polarities in order to better describe the chemical compounds present. In negative mode, the HESI source data were compared to the APCI data (Tables 2 and 3), showing an increase of the number of chemical formulae detected by 20 to 30%. This

increase is characterized by a better detection of negatively ionized chemical compounds and those with a higher unsaturation number (DBE). In order to evaluate further the interest for using these ionization sources, we compiled these data in Venn diagrams and proposed a visualization of these sets with a van Krevelen representation; we added the number of DBE in the third dimension. These results are presented in Tables 2 and 3.

In positive ionization mode, independently of the ionization source and in addition to the common molecular formulae, we detected chemical compounds with an O/C ratio < 0.2 whereas in the negative ionization mode, we detected molecular formulae with an O/C ratio > 0.5. In addition to these observations, we noted that HESI is more appropriate for studying chemical compounds with a large number of unsaturation (DBE > 5). Finally, for an optimal detection of the oxidation chemical compounds, it is necessary to consider the transmission limits of the C-Trap. Here, we could increase by more than 60% the number of molecular formulae detected using several mass ranges for data acquisition. The most appropriate ionization polarity to be used is tight to chemical functions present in chemical compounds to be detected. We could increase by 30 to 100% the number of chemical formulae detected by using both positive and negative ionization modes. The ionization source used is also important. We could increase the number of detected chemical formulae by 20 to 30% using HESI. We believe that this approach to data validation and these results, although specific to this study, are applicable to any characterization by Orbitrap. To illustrate the present results, spectra of AP and LM acquired with a HESI source in negative mode are given in supplement (Fig. S1).

**Table 2.** Representation of the mass spectrometry data characterizing the oxidation of AP and LM (ionization source: APCI positive and negative mode, JSR experiments). Enlarged formats of the 3D graphs are presented in supplement S2.

| | **α-Pinene** | | | **Limonene** | | |
|---|---|---|---|---|---|---|
| Source and mode | **APCI$^+$** | | **APCI$^-$** | **APCI$^+$** | | **APCI$^-$** |
| Number of compounds | 646 | | 503 | 1321 | | 1346 |
| Distribution | specific to positive mode 327 | common 319 | specific to negative mode 174 | specific to positive mode 516 | common 805 | specific to negative mode 542 |
| Venn graph | 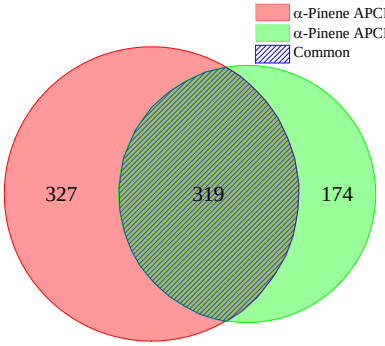 Total : 820 | | | 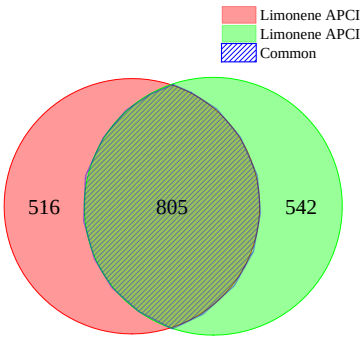 Total :1863 | | |
| VK *vs* DBE | 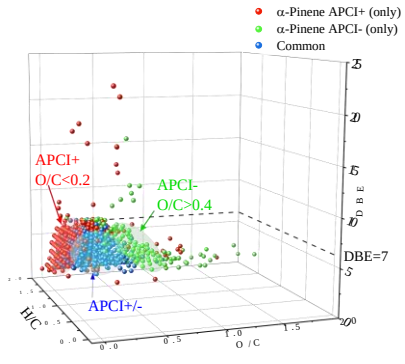 | | | 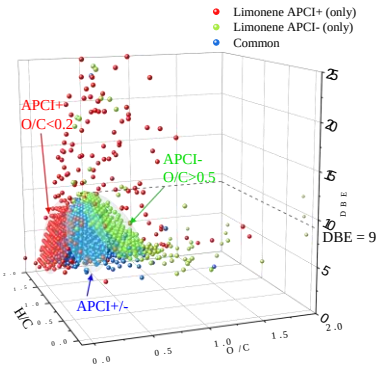 | | |
| | 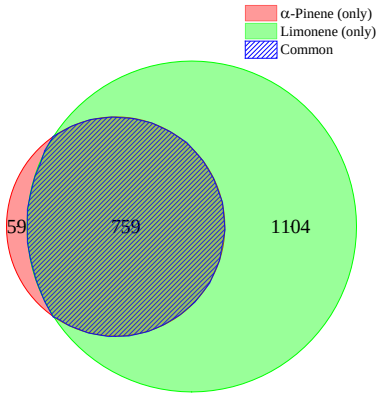 Total : 1920 | | | 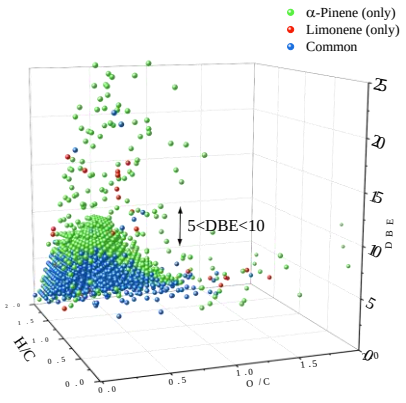 | | |

**Table 3.** Representation of the mass spectrometry data characterizing the oxidation of α-pinene and limonene (ionization source: HESI positive and negative modes, JSR experiments). Enlarged formats of the 3D graphs are presented in supplement S3.

| | **α-Pinene** | | | **Limonene** | | |
|---|---|---|---|---|---|---|
| Source and mode | **HESI$^+$** | | **HESI$^-$** | **HESI$^+$** | | **HESI$^-$** |
| Number of compounds | 594 | | 603 | 1017 | | 1864 |
| Distribution | specific to positive mode 282 | common 312 | specific to negative mode 381 | specific to positive mode 353 | common 482 | specific to negative mode 1342 |
| Venn Graph | 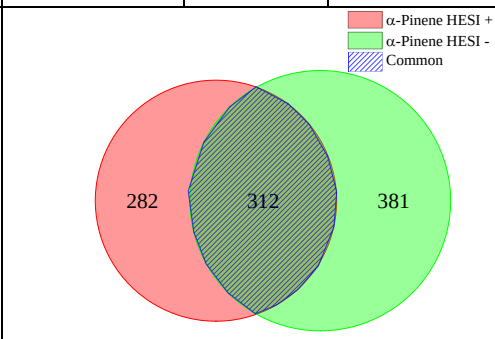 Total : 975 | | | 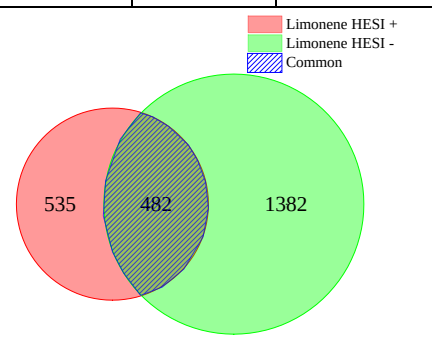 Total : 2399 | | |
| VK *vs* DBE | 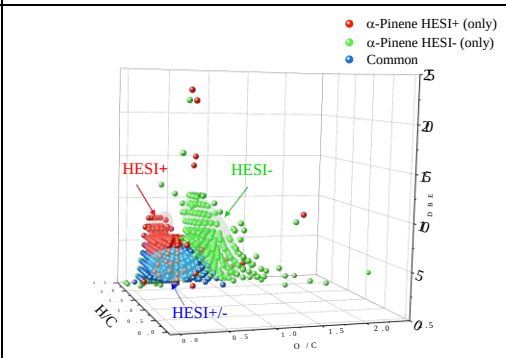 | | | 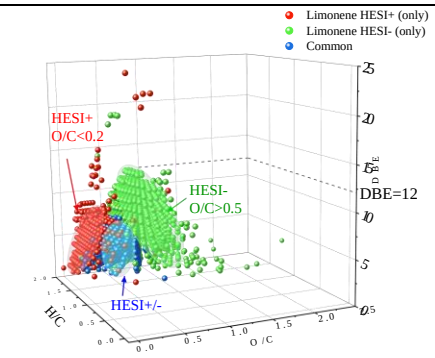 | | |
| | 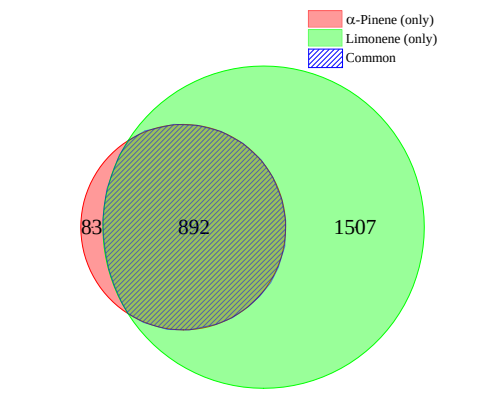 Total : 2482 | | | 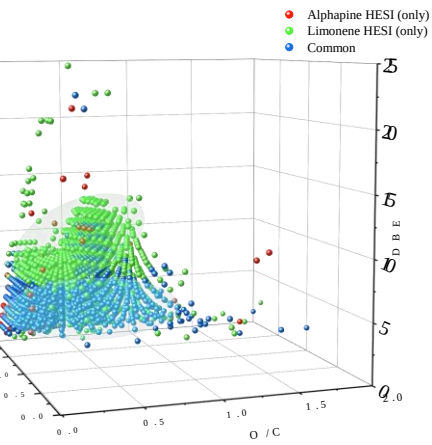 | | |

### 4.2 Autoxidation chemical compounds detected in a JSR

In order to compare the oxidation of AP and LM, we compiled the positive and negative ionization data obtained with APCI (Table 2) and HESI (Table 3) ionization sources to obtain a more exhaustive database. For the APCI and HESI sources, we distinguished three datasets, two of which are specific to the oxidation of AP and LM and one which is common to both isomers. In the following, the name "only" will be used to describe the molecules specific to the oxidation of one of the terpenes. This common dataset represents more than 90% of the chemical formulae identified in AP oxidation samples, detected with both APCI and HESI. For LM, where the number of identified chemical formulae is greater, this common dataset ranges between 68% in APCI and 37% in HESI. In these two cases, the relatively low residence time (2 seconds) and the diversity of the chemical formulae obtained show that the oxidation of these two terpenes leads to the opening of the ring, a phenomenon also observed in atmospheric chemistry (Berndt et al., 2016;Zhao et al., 2018;Iyer et al., 2021). Concerning the molecular formulae common to both terpenes, Figure 1 shows that they are limited to 10 oxygen atoms. This limit is linked to AP whose oxidation beyond 10 oxygen atoms remains low (less than 2% of the totality of the observed chemical formulae for this terpene). The autoxidation will allow keeping this similarity in the different steps of the oxidation by simple addition of two atoms of oxygen. In the case of LM, the presence of an exocyclic double bond will increase, in a similarly to atmospheric chemistry conditions (Kundu et al., 2012), the possibilities of oxidation and accretion. It remains however impossible, considering the size of the sets and the diversity of the isomers, to formalize all the reaction mechanisms. Nevertheless, the formation of oxidized chemical compounds can be described with the help of graphical tools. The dispersion of the number of oxygen atoms per molecule shows for example that LM oxidizes more than AP (Tables 2 and 3). In the case of LM, using a HESI source, an oxygen number of up to 15 is measured, with maximum counts recorded for 10 O-atoms (Fig. 1), whereas it remains mostly less than or equal to 10 for AP (Fig. 1). Moreover, this graph shows, for the chemical compounds specific of LM oxidation, a distribution centered on 11 oxygen atoms with carbon skeletons probably resulting from accretion.

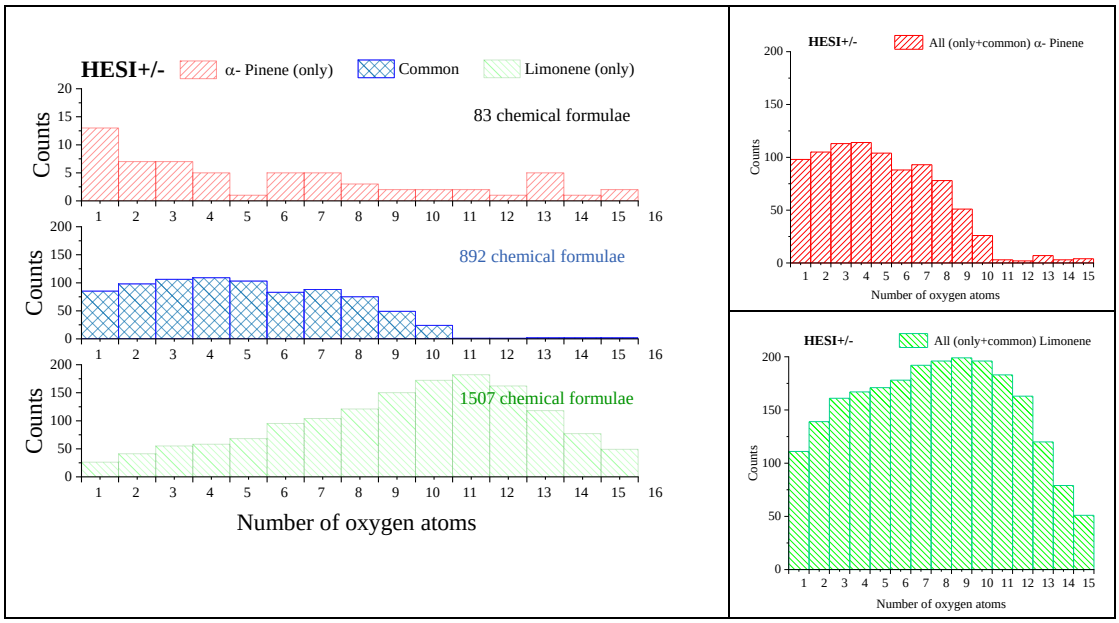


**Figure 1:** Distribution of AP and LM autoxidation chemical compounds as a function of their oxygen content (ionization source: HESI, combined positive and negative modes data).

To verify this accretion hypothesis, we can plot the OSc as a function of the number of carbon atoms or the O/C ratio at fixed number of C-atoms (Fig. 2). One can visualize the evolution of the molecular oxidation for each carbon skeleton and the formation of oligomers. Chemical compounds which are unique to one of the isomers, or common to both are differentiated using different colors. In addition to the autoxidation represented by the vertical axes for a given number of carbon atoms (Fig. 2a), we observe mechanisms of fragmentation, accretion and oligomerization between the carbon skeleton. These reaction mechanisms contribute to forming families according to the rate of oxidation and the size of their carbon skeleton. The increase in the number of oxygen atoms, but also of carbon atoms will decrease chemical compounds volatility. We distinguish four families: low volatile oxygenated organic aerosols (LV-OOA), semi-volatile oxygenated organic aerosols (SV-OOA), biomass burning organic aerosols (BBOA) and water-soluble organic carbons (WSOC) following a classification proposed in the literature (Kroll et al., 2011). If we analyze the two sets of molecules from the APCI and HESI sources, positive and negative ionization modes combined, we find that nearly 73% of the molecules are linked to each other by a single difference of 2 oxygen atoms which reflects an autoxidation mechanism (Fig. 3).

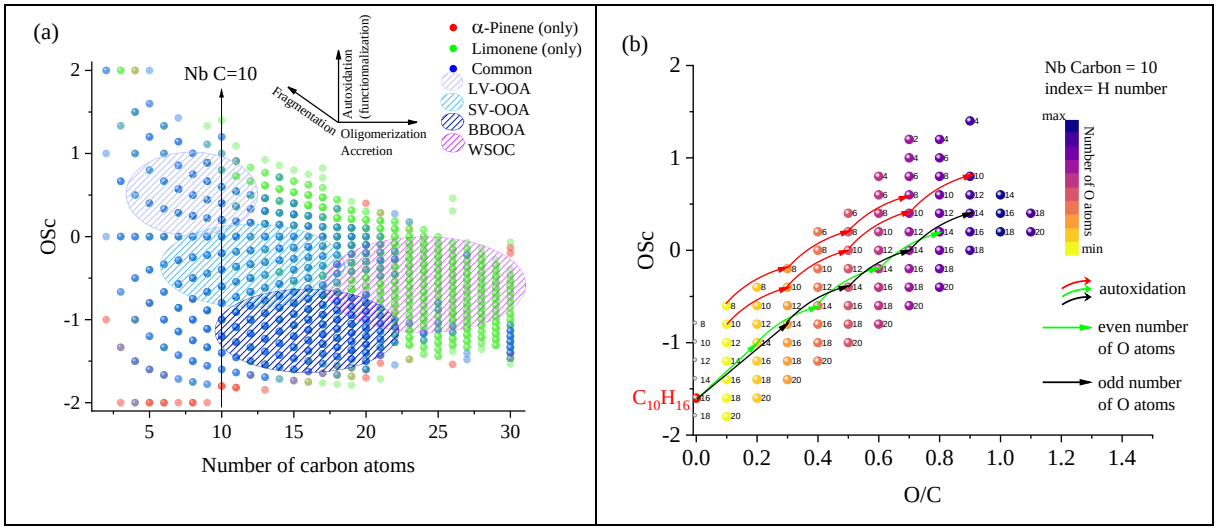


**Figure 2:** Overview of the distribution of LM and AP oxidation chemical compounds observed in a JSR: (a) OSc versus carbon number in detected chemical formulae from APCI and HESI data. (b) OSc versus O/C atomic ratio for a carbon number of 10; index of the chemical compounds: number of hydrogen atoms. Arrows indicate autoxidation from a $C_6H_{16}$ isomer, according to the oxygen parity in chemical compounds.

We can measure the amplitude of autoxidation for each carbon skeleton from the OSc vs. O/C space. For the two terpenes, for which the initial carbon number (C) is equal to 10, one can observe (Fig. 2b) two autoxidation routes with an even and odd number of oxygen atoms. This parity distinction is initially present for the two main radicals, ROO˙ and RO˙, responsible for autoxidation. However, the termination and propagation reactions will change the oxygen parity to form a new distribution where the parity links between radicals and molecules are lost, making any interpretation of radicals oxidation route impossible (Fig. 3). The autoxidation mechanisms indicated by arrows in Figure 2b characterize systematic peroxy chain terminations which do not change oxygen parity. HESI data showed an equivalent distribution of the two oxygen parities in chemical compounds (odd: 51%; even 49%) therefore confirming a lack of selectivity of the reaction mechanisms with respect to the parity of the radicals.

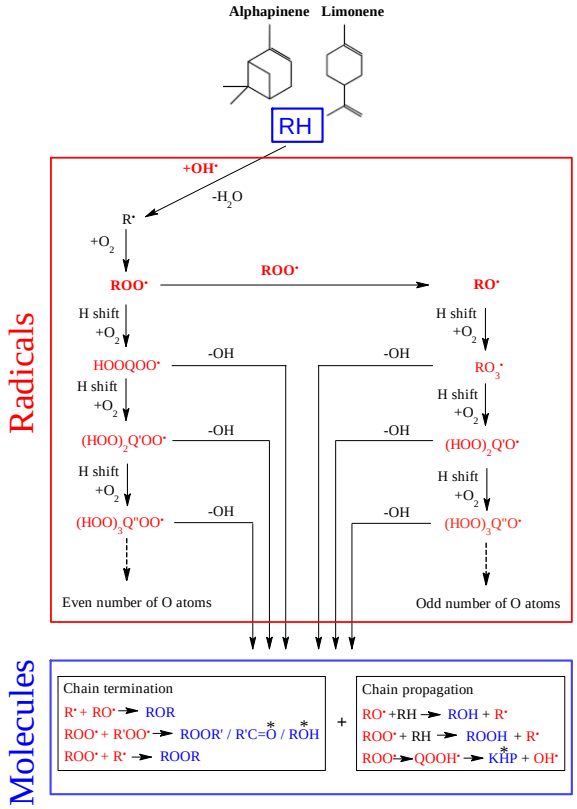


**Figure 3:** Autoxidation reaction mechanisms in combustion (left) and in the atmosphere (left and right). * indicates a change in number of oxygen atoms.

### 4.3 Combustion versus atmospheric oxidation

We have explored potential chemical pathways related to autoxidation in the previous section. For this purpose, we have performed experiments under cool flame conditions (590 K). This autoxidation mechanism is also present in atmospheric chemistry, but it is only recently that it has been found that this mechanism could be one of the main formation pathways for SOA (Savee et al., 2015). Studies have described this mechanism in the case of atmospheric chemistry with the identification of radicals and molecular compounds (Tomaz et al., 2021). However, previous studies mainly focused on the initial skeletons of the 10-carbon terpenes, whereas the other carbon skeletons are also concerned by autoxidation. It is therefore useful to evaluate the proportion of chemical compounds of autoxidation among the total chemical compounds formed.

We propose a new approach which consists in assessing a set of molecules mainly resulting from autoxidation against different sets of experimental studies related to atmospheric chemistry. The objective is to compare the similarity between these conditions on the basis of autoxidation by considering different experimental parameters chosen for their diversity. For this purpose, we selected, a HESI ionization source, better adapted to the electronegativity of the oxidized molecules, as well as to higher *m/z*. Moreover, we have already shown in this paper that the HESI (+/-) ionization source is better suited for detecting autoxidation chemical compounds (detection of 96% of the total chemical formulae observed in autoxidation).

Among published atmospheric chemistry studies of terpenes oxidation, we have selected 15 studies, 4 for AP and 11 for LM. The data were acquired using different experimental procedures (methods of oxidation, techniques of characterization). Table 4 summarizes all the experimental parameters of the selected studies.

318 **Table 4.** Experimental settings of 15 oxidation studies of two terpenes under atmospheric conditions and cool
319 flames.

| Reference | Oxidation mode | Sampling | Experimental setup | Concentrations of reactants | Ionization /source | Instrument | Chemical formulae |
|---|---|---|---|---|---|---|---|
| **α-Pinene** | | | | | | | |
| Y. Deng et al. (2021) | Dark ozonolysis seed particles OH scavenger | online | Teflon bag; 0.7m3 | 3.3±0.6 ncps $ppbv^{-1}$ AP | ESI | ToF-MS | 351 |
| Quéléver et al. (2019) | Ozonolysis | online | Teflon bag 5 $m^3$ | 10 & 50 ppb AP | $NO_3^-$ (CI) | CI-APi-TOF | 68 |
| Meusinger et al. (2017) | Dark Ozonolysis OH scavenger no seed particles | offline | Teflon bag 4.5 $m^3$ | 60 ppb AP | Proton transfer | PTR-MS-ToF | 153 |
| Krechmer at al. (2016) | Ozonolysis | offline | PAM Oxidation reactor | Field measurement | ESI (-) and $NO_3^-$ (CI) | CI-IMS-ToF | 43 |
| This work | Cool-flame autoxidation | offline | jet-stirred reactor | 1%, AP No ozone | APCI(3kV) HESI (3kV) | Orbitrap® Q-Exactive | 820 (APCI) 975 (HESI) |
| **Limonene** | | | | | | | |
| Krechmer et al. (2016) | Ozonolysis | offline | PAM Oxidation reactor | not specified | ESI (-) and $NO_3^-$ (CI) | CI-IMS-ToF | 63 |
| Tomaz et al. (2021) | Ozonolysis | online | flow tube reactor (18 L) | 45-227 ppb LM | $NO_3^-$ (CI) - Neg | Orbitrap® Q-Exactive | 282 |
| Fang et al. (2017) | OH-initiated photooxidation dark ozonolysis | online | smog chamber | 900–1500 ppb LM | UV; 10 eV | Time-of-Flight (ToF) | 17 |
| Witkowski and Gierczak (2017) | Dark ozonolysis | offline | flow reactor | 2 ppm, LM | ESI,4.5 kV | Triple quadrupole | 12 |
| (Jokinen et al., 2015b) | Ozonolysis | online | flow glass tube | 1–10000 $x10^9$ $molec.cm^{-3}$, LM | chemical ionization | Time-of-Flight (ToF) | 11 |
| Nørgaard et al. (2013) | Ozone (plasma) | online | direct on the support | 850 ppb ozone 15-150 ppb LM | plasma | Quadrupole time-of-flight (QToF) | 29 |
| Bateman et al. (2009) | Dark and UV radiations ozonolysis | offline | Teflon FEP reaction chamber | 1 ppm ozone 1 ppm LM | modified ESI (+/-) | LTQ-Orbitrap Hybrid Mass (ESI) | 924 |
| Walser et al. (2008) | Dark ozonolysis | offline | Teflon FEP reaction chamber | 1-10 ppm ozone 10 ppm LM | ESI (+/-); 4.5 kV | LTQ-Orbitrap Hybrid Mass (ESI) | 465 |
| Warscheid and Hoffmann (2001) | Ozonolysis | online | Smog chamber | 300-500 ppb LM | APCI; 3kV | Quadrupole ion trap mass | 21 |
| Hammes et al., (2019) | Dark ozonolysis | online | flow reactor | 15, 40, 150 ppb LM | $^{210}$ Po α- | HR-ToF-CIMS | 20 |
| Kundu et al. (2012) | Dark ozonolysis | offline | Teflon reaction chamber | 250 ppb ozone 500 ppb LM | ESI; 3.7 and 4 kV | LTQ FT Ultra, Thermo Sct (ESI) | 1199 |
| This work | Cool-flame autoxidation | offline | jet-stirred reactor | 1%, LM No ozone | APCI(3kV) HESI (3kV) | Orbitrap® Q-Exactive | 1863(APCI) 2399(HESI) |

320

The data are from the articles or files provided in the Supplementary S4. In these studies, oxidation was performed mostly by ozonolysis (Fang et al., 2017) with different experimental conditions that gather the main methods described in the literature: ozonolysis, dark ozonolysis, ozonolysis with OH scavenger, ozonolysis with or without seed particles. We considered that the methods of analysis by mass spectrometry did not modify the nature of the chemical species but only their relative importance, because of the type of ionization and the sensitivity of the instruments. The combination of data obtained using (+/-) HESI gives a rather complete picture of the autoxidation chemical compounds.

First, we compared the data from ozonolysis studies of each terpene and identified similarities through a Venn diagram. For studies with two ionization sources, duplicate chemical formulae were removed. We selected the three most representative studies, by the number of chemical formulae detected. Then, we compared the set of chemical formulae identified after ozonolysis to those produced in low-temperature combustion. The objective was (i) to highlight similarities in terms of chemical compounds generated by the two oxidation modes and (ii) to identify data resulting from autoxidation.

For AP oxidation, the four studies identified 566 chemical formulae, all polarities combined. Only the study by (Meusinger et al., 2017) was performed in positive mode and none of the studies reported data obtained with two ionization modes (+/–). For LM oxidation, the three studies identified 1862 chemical formulae. Only the studies by (Walser et al., 2008;Bateman et al., 2009) used (+) and (–) ionization modes. In the case of LM oxidation, for which accretion is more important than for AP, and for which a greater number of chemical formulae were identified, the similarity is more important. These results are presented in Figure 4 where the ionization polarity used in each study is specified.

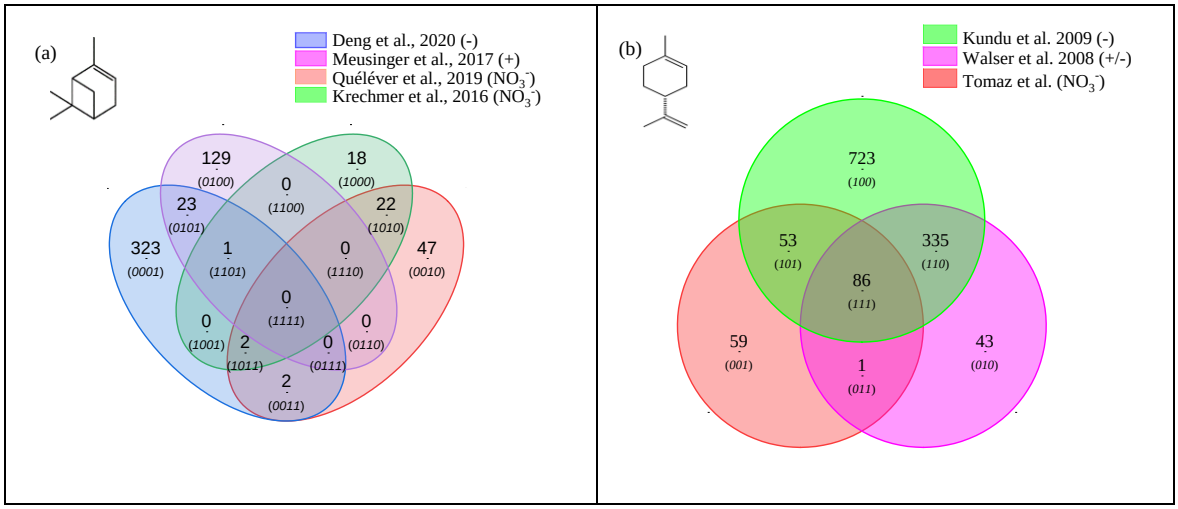


**Figure 4:** Venn diagrams comparing the oxidation results from ozonolysis of (a) AP and (b) LM (see conditions in Table 1). Each digit of the binary numbers in parentheses identifies the datasets being compared.

For α-pinene, no global similarity is observed for the detected chemical formulae. Different hypotheses can be offered to explain this result. Among them, the number of chemical formulae identified per study remains limited (a few dozen to several hundreds) and these small datasets are sometimes restricted to specific mass ranges (e.g. $C_{10}$ to $C_{20}$ (Quéléver et al., 2019)). In the case of studies carried out with an $NO_3^-$ source, sensitive to HOMS,

produced preferentially by autoxidation, we note that nearly 50% of the chemical formulae (10/22) are linked by a simple difference of 2 oxygen atoms.

For LM, 86 chemical formulae are common to the three studies considered here. In this dataset, nearly 43% of the chemical formulae present a relation similar to that of autoxidation (simple difference of two oxygen atoms) with less than 5% of fragments (Nb C<10). This result seems to indicate that autoxidation dominates.

Then, one can ask if reaction mechanisms common to atmospheric and combustion chemistry can generate, despite radically different experimental conditions, a set of common chemical formulae and if in this common dataset, a common link, characteristic of autoxidation, is observable?

To address that question, we compared all the previous results, for AP and LM to those obtained under the present combustion study. The comparisons were made using HESI data. One should remember that the oxidation conditions in a JSR were chosen in order to maximize low-temperature autoxidation. Again, we used Venn diagrams to analyze these datasets composed of 1590 chemical formulae in the case of AP and 2857 chemical formulae in the case of LM. The results of these analyses are presented in Figure 5.

It turned out that 301 chemical formulae for AP and 735 chemical formulae for LM were identified to be common to oxidation by ozonolysis and combustion. This represents 31% of the chemical formulae for the ozonolysis of AP and 31% for those of LM ozonolysis. For AP, the similarities compared to combustion are specific to each study: 69% (Deng et al., 2021), 46% (Meusinger et al., 2017), 7% (Quéléver et al., 2019), 23% (Krechmer et al., 2016). Chemical formulae common to all studies were not identified. This may be due to a partial characterization of the chemical formulae, a weaker oxidation of AP with an ionization mode less favorable to low molecular weights.

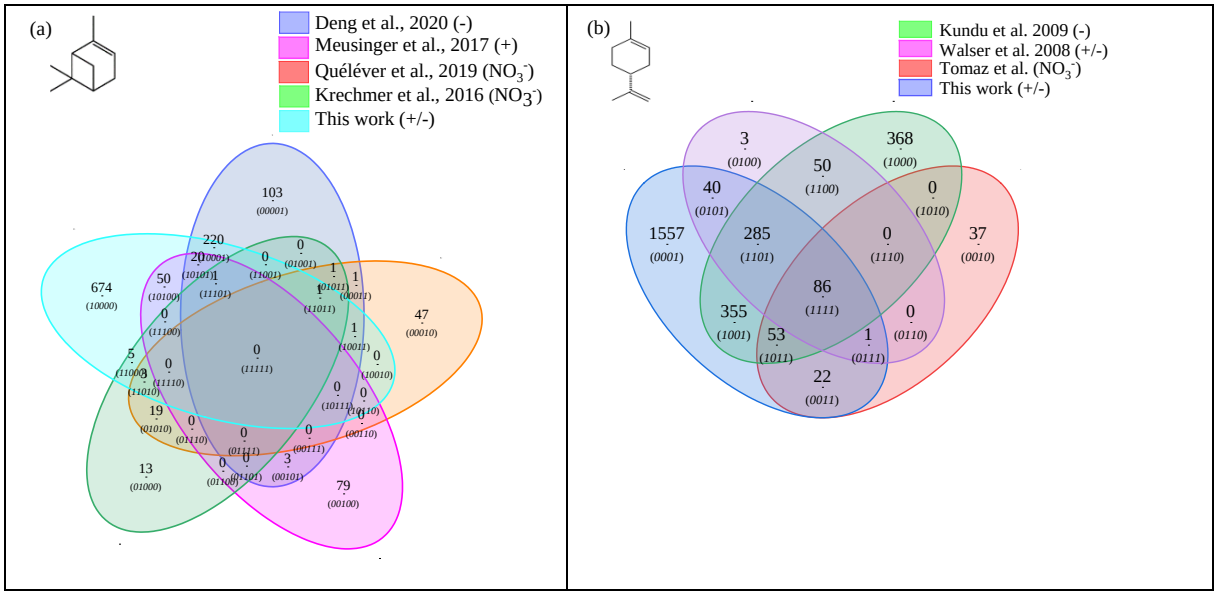


**Figure 5:** Venn diagrams comparing the oxidation results from ozonolysis and combustion of (a) AP and (b) LM (see conditions in Table 1).

For LM, the similarities between oxidation by ozonolysis and combustion are more important and less spread out. They represent for the different studies: 65% (Kundu et al., 2012), 88% (Walser et al., 2008), 81% (Tomaz et al.,

2021). Moreover, there is a common dataset of 86 chemical formulae which can derive from autoxidation mechanisms. Whereas different reaction mechanisms can cause the observed similarities, the preponderance of autoxidation in cool flame combustion is obvious (Affleck and Fish, 1967;Fish, 1968). In atmospheric chemistry, this reaction mechanism remains competitive or dominates (Crounse et al., 2013;Jokinen et al., 2014b). If we search for an autoxidation link between these 86 chemical formulae, i.e., $C_nH_mO_x$ to $C_nH_mO_{x+2}$, we observe that 40% of these chemical formulae meet this condition (Fig. 6b). Indeed, a difference of two oxygen atoms, at constant number of carbon and hydrogen atoms is observed. In order to visualize the 'autoxidation' links between these chemical compounds, a three dimensional graph is presented in the Supplements (Fig S5). More precisely, these molecules are centered in a van Krevelen diagram on the ratios O/C=0.6 and H/C=1.6, in the range 0.25 < O/C < 0.8 and 1.25 < H/C < 1.85. All oxidized molecules associated with this dataset are presented in Figure 6. The dispersion of the chemical formulae, far from being random, remains consistent with an autoxidation mechanism where the number of carbon atoms is constant.

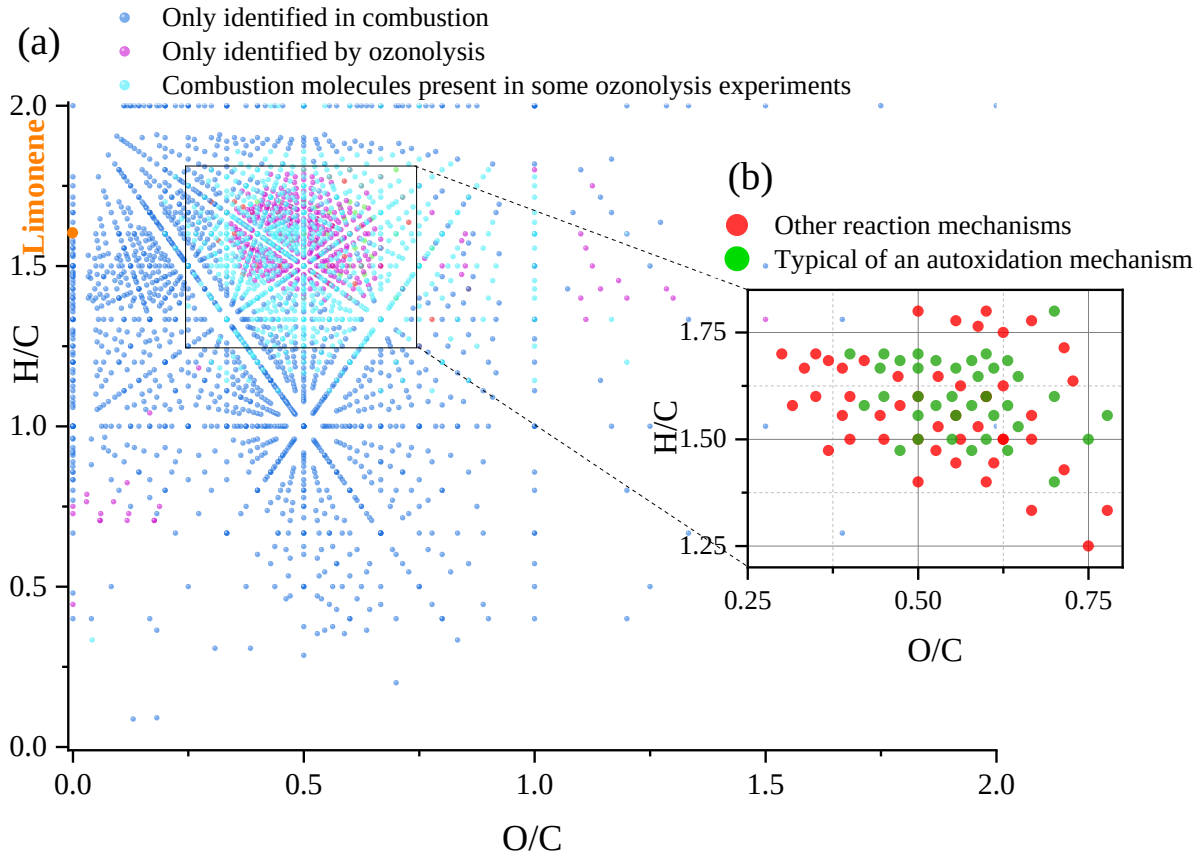


**Figure 6:** Van Krevelen diagram showing (a) specific and common chemical formulae detected after the oxidation of LM by ozonolysis and combustion and (b) the 86 chemical formulae common to all studies.

A 3-D representation of all LM oxidation data is given in Fig. S6 (Supplement) where DBE is used as third dimension. From that figure, one can note that chemical compounds with higher DBE are preferably formed under JSR conditions, i.e. at elevated temperature. These chemical formulae could correspond to carbonyls and / or cyclic ethers (•QOOH → carbonyl + alkene + OH and / or cyclic ether + OH).

Specificities and similarities of these two oxidation modes were further investigated by plotting the distribution of the number of oxygen atoms in detected chemical formulae (Fig. 7). Indeed, the distribution of the number of oxygen atoms allows, in addition to the Van Krevelen diagram, to provide some additional details on these two modes of oxidation. It is in ozonolysis that we observe the chemical formulae having the largest number of oxygen atoms. There, oxidation proceeds over a long reaction time where the phenomenon of aging appears by promoting accretion or oligomerization. Whereas a short residence time (2 s) was used in JSR experiments. A short residence time should limit accretion which is favored under simulated atmospheric oxidation experiments performed over long reaction times. In combustion, the number of oxygen atoms remains limited to 18, with a lower number of detected chemical formulae compared to the case of ozonolysis. However, it is in combustion that we observe the highest O/C ratios, indicating the formation of the most oxidized chemical compounds. This difference, however, does not affect the similarities between the chemical formulae detected in the two modes of oxidation. Finally, the analysis of the parities in oxygen atoms, very similar in the three datasets, confirms that the reaction mechanisms presented in Figure 3 do not allow a simple link to be established between the parity of radicals and that of chemical compounds.

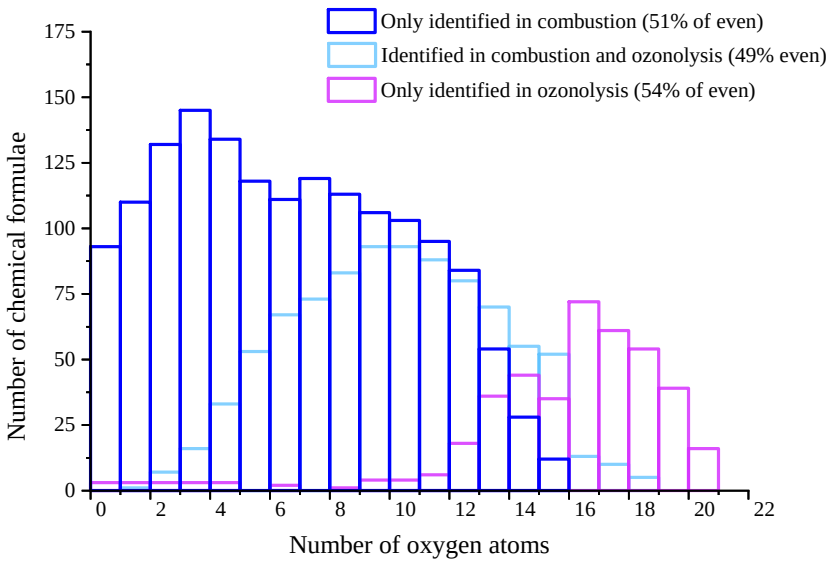


**Figure 7:** Oxygen number distribution for all the molecules identified for the oxidation of LM: only in combustion, only in ozonolysis and common to both processes. For each of these distributions, the parity in oxygen number is specified

### 4.3 Atmosphere implication

While this study has shown similarities in oxidation chemistries under atmospheric and cool flame conditions, and considering recent findings in biomass burning (Smith et al., 2009) and large wildfires (Khaykin et al., 2020;Ohneiser et al., 2020) studies, it would be interesting to apply and extend the analytical procedure developed in the present work to other chemical systems. One could investigate the chemical reaction mechanisms involved in biomass burning. For example, it has been reported (Smith et al., 2009) the detection of HOMs in aerosol samples generated by biomass burning, consistent with

other measurements (Oros and Simoneit, 2001;Hays et al., 2002;Mazzoleni et al., 2007;Iinuma et al., 2007). One could then propose potential chemical compounds to be tracked, e.g., in tropospheric field measurements and in balloon-borne air sampling since biomass burning aerosols can be transported far from their emission area and to high altitude.

## 5 Conclusion

We have analyzed and compared, thanks to different mathematical and visualization tools, the oxidation of AP and LM under simulated tropospheric and cool flame oxidation conditions. We have restricted the field of this study to organic compounds ($C_nH_yO_z$) in order to study specifically autoxidation. This work is in the continuity of recently published studies which established the importance of autoxidation under tropospheric oxidation and low-temperature combustion conditions. Faced with the analytical limits of the chemical speciation of thousands of molecules, and in order to complete the work carried out on the reaction mechanisms of the first steps of oxidation, we have developed a global approach based on the study of families of chemical compounds present in these large sets (van Krevelen diagram, oxygen number distribution, oxidation state of carbon -OSc, chemical relationship between molecules). We selected existing databases on ozonolysis with a purposive diversity of experimental conditions and compared these data to those obtained in low-temperature combustion conditions where autoxidation is important (cool flame combustion at 590 K). We showed that a significant portion of the chemical compounds were common to both atmospheric and combustion products. Surprisingly, the numerous oxidation mechanisms and the isomerization of chemical compounds proceeding under these two conditions did not lead to diverging data, but, on the contrary, to similarities. More than 40% of the chemical formulae detected in combustion chemistry experiments using a JSR have been detected in the studies carried out under atmospheric conditions. Finally, we have outlined the existence of a substantial common dataset of autoxidation products. This result tends to show that autoxidation is indeed inducing similarity between atmospheric and combustion chemical compounds. This work could be extended by studying in detail, the formation of HOMs during, biomass fire reported earlier (Smith et al., 2009).

## Acknowledgements

The authors gratefully acknowledge funding from the Labex Caprysses (ANR-11-LABX-0006-01), the Labex Voltaire (ANR-10-LABm/zX-100-01), CPER, and EFRD (PROMESTOCK and APPROPOR-e projects). We also thank Matthieu RIVA for sharing his experimental data on LM oxidation.

## References

Affleck, W. S., and Fish, A.: Two-stage ignition under engine conditions parallels that at low pressures, Symposium (International) on Combustion, 11, 1003-1013, 10.1016/S0082-0784(67)80227-3, 1967.

Andreae, M. O.: Emission of trace gases and aerosols from biomass burning – an updated assessment, Atmos. Chem. Phys., 19, 8523-8546, 10.5194/acp-19-8523-2019, 2019.

Barsanti, K. C., Kroll, J. H., and Thornton, J. A.: Formation of Low-Volatility Organic Compounds in the Atmosphere: Recent Advancements and Insights, J Phys Chem Lett, 8, 1503-1511, 10.1021/acs.jpclett.6b02969, 2017.

Bateman, A. P., Nizkorodov, S. A., Laskin, J., and Laskin, A.: Time-resolved molecular characterization of limonene/ozone aerosol using high-resolution electrospray ionization mass spectrometry, Physical Chemistry Chemical Physics, 11, 7931-7942, 10.1039/B905288G, 2009.

Belhadj, N., Benoit, R., Dagaut, P., Lailliau, M., Serinyel, Z., Dayma, G., Khaled, F., Moreau, B., and Foucher, F.: Oxidation of di-n-butyl ether: Experimental characterization of low-temperature products in JSR and RCM, Combustion and Flame, 222, 133-144, 10.1016/j.combustflame.2020.08.037, 2020.

Belhadj, N., Lailliau, M., Benoit, R., and Dagaut, P.: Experimental and kinetic modeling study of n-hexane oxidation. Detection of complex low-temperature products using high-resolution mass spectrometry, Combustion and Flame, 233, 111581, 10.1016/j.combustflame.2021.111581, 2021.

Benoit, R., Belhadj, N., Lailliau, M., and Dagaut, P.: On the similarities and differences between the products of oxidation of hydrocarbons under simulated atmospheric conditions and cool flames, Atmos. Chem. Phys., 21, 7845-7862, 10.5194/acp-21-7845-2021, 2021.

Berndt, T., Richters, S., Kaethner, R., Voigtländer, J., Stratmann, F., Sipilä, M., Kulmala, M., and Herrmann, H.: Gas-Phase Ozonolysis of Cycloalkenes: Formation of Highly Oxidized RO2 Radicals and Their Reactions with NO, NO2, SO2, and Other RO2 Radicals, The Journal of Physical Chemistry A, 119, 10336-10348, 10.1021/acs.jpca.5b07295, 2015.

Berndt, T., Richters, S., Jokinen, T., Hyttinen, N., Kurtén, T., Otkjær, R. V., Kjaergaard, H. G., Stratmann, F., Herrmann, H., Sipilä, M., Kulmala, M., and Ehn, M.: Hydroxyl radical-induced formation of highly oxidized organic compounds, Nature Communications, 7, 13677, 10.1038/ncomms13677, 2016.

Bianchi, F., Kurtén, T., Riva, M., Mohr, C., Rissanen, M. P., Roldin, P., Berndt, T., Crounse, J. D., Wennberg, P. O., Mentel, T. F., Wildt, J., Junninen, H., Jokinen, T., Kulmala, M., Worsnop, D. R., Thornton, J. A., Donahue, N., Kjaergaard, H. G., and Ehn, M.: Highly Oxygenated Organic Molecules (HOM) from Gas-Phase Autoxidation Involving Peroxy Radicals: A Key Contributor to Atmospheric Aerosol, Chemical Reviews, 119, 3472-3509, 10.1021/acs.chemrev.8b00395, 2019.

Chen, J., Li, C., Ristovski, Z., Milic, A., Gu, Y., Islam, M. S., Wang, S., Hao, J., Zhang, H., He, C., Guo, H., Fu, H., Miljevic, B., Morawska, L., Thai, P., Lam, Y. F., Pereira, G., Ding, A., Huang, X., and Dumka, U. C.: A review of biomass burning: Emissions and impacts on air quality, health and climate in China, Science of The Total Environment, 579, 1000-1034, 10.1016/j.scitotenv.2016.11.025, 2017.

Crounse, J. D., Nielsen, L. B., Jørgensen, S., Kjaergaard, H. G., and Wennberg, P. O.: Autoxidation of organic compounds in the atmosphere, J. Phys. Chem. Lett., 4, 3513, 2013.

Dagaut, P., Cathonnet, M., Rouan, J. P., Foulatier, R., Quilgars, A., Boettner, J. C., Gaillard, F., and James, H.: A jet-stirred reactor for kinetic studies of homogeneous gas-phase reactions at pressures up to ten atmospheres (≈1 MPa), Journal of Physics E: Scientific Instruments, 19, 207-209, 10.1088/0022-3735/19/3/009, 1986.

Dagaut, P., Cathonnet, M., Boetiner, J. C., and Gaillard, F.: Kinetic Modeling of Propane Oxidation, Combustion Science and Technology, 56, 23-63, 10.1080/00102208708947080, 1987.

Dagaut, P., Cathonnet, M., Boettner, J. C., and Gaillard, F.: Kinetic modeling of ethylene oxidation, Combustion and Flame, 71, 295-312, 10.1016/0010-2180(88)90065-X, 1988.

Deng, Y., Inomata, S., Sato, K., Ramasamy, S., Morino, Y., Enami, S., and Tanimoto, H.: Temperature and acidity dependence of secondary organic aerosol formation from α-pinene ozonolysis with a compact chamber system, Atmos. Chem. Phys., 21, 5983-6003, 10.5194/acp-21-5983-2021, 2021.

Fang, W., Gong, L., and Sheng, L.: Online analysis of secondary organic aerosols from OH-initiated photooxidation and ozonolysis of α-pinene, β-pinene, Δ3-carene and d-limonene by thermal desorption–photoionisation aerosol mass spectrometry, Environmental Chemistry, 14, 75-90, 10.1071/EN16128, 2017.

Fawaz, M., Avery, A., Onasch, T. B., Williams, L. R., and Bond, T. C.: Technical note: Pyrolysis principles explain time-resolved organic aerosol release from biomass burning, Atmos. Chem. Phys., 21, 15605-15618, 10.5194/acp-21-15605-2021, 2021.

Fish, A.: The Cool Flames of Hydrocarbons, Angewandte Chemie International Edition in English, 7, 45-60, 10.1002/anie.196800451, 1968.

Hammes, J., Lutz, A., Mentel, T., Faxon, C., and Hallquist, M.: Carboxylic acids from limonene oxidation by ozone and hydroxyl radicals: insights into mechanisms derived using a FIGAERO-CIMS, Atmos. Chem. Phys., 19, 13037-13052, 10.5194/acp-19-13037-2019, 2019.

Hays, M. D., Geron, C. D., Linna, K. J., Smith, N. D., and Schauer, J. J.: Speciation of Gas-Phase and Fine Particle Emissions from Burning of Foliar Fuels, Environmental Science & Technology, 36, 2281-2295, 10.1021/es0111683, 2002.

Hecht, E. S., Scigelova, M., Eliuk, S., and Makarov, A.: Fundamentals and Advances of Orbitrap Mass Spectrometry, in: Encyclopedia of Analytical Chemistry, 1-40, 2019.

Huang, W., Saathoff, H., Pajunoja, A., Shen, X., Naumann, K. H., Wagner, R., Virtanen, A., Leisner, T., and Mohr, C.: α-Pinene secondary organic aerosol at low temperature: chemical composition and implications for particle viscosity, Atmos. Chem. Phys., 18, 2883-2898, 10.5194/acp-18-2883-2018, 2018.

Iinuma, Y., Brüggemann, E., Gnauk, T., Müller, K., Andreae, M. O., Helas, G., Parmar, R., and Herrmann, H.: Source characterization of biomass burning particles: The combustion of selected European conifers, African hardwood, savanna grass, and German and Indonesian peat, Journal of Geophysical Research: Atmospheres, 112, 10.1029/2006JD007120, 2007.

Iyer, S., Rissanen, M. P., Valiev, R., Barua, S., Krechmer, J. E., Thornton, J., Ehn, M., and Kurtén, T.: Molecular mechanism for rapid autoxidation in α-pinene ozonolysis, Nature Communications, 12, 878, 10.1038/s41467-021-21172-w, 2021.

Jokinen, T., Sipilä, M., Richters, S., Kerminen, V.-M., Paasonen, P., Stratmann, F., Worsnop, D., Kulmala, M., Ehn, M., Herrmann, H., and Berndt, T.: Rapid Autoxidation Forms Highly Oxidized RO2 Radicals in the Atmosphere, Angewandte Chemie International Edition, 53, 14596-14600, 10.1002/anie.201408566, 2014a.

Jokinen, T., Sipila, M., Richters, S., Kerminen, V. M., Paasonen, P., Stratmann, F., Worsnop, D., Kulmala, M., Ehn, M., and Herrmann, H.: Rapid autoxidation forms highly oxidized RO2 radicals in the atmosphere, Angew. Chem., Int. Ed., 53, 14596, 2014b.

Jokinen, T., Berndt, T., Makkonen, R., Kerminen, V.-M., Junninen, H., Paasonen, P., Stratmann, F., Herrmann, H., Guenther, A. B., Worsnop, D. R., Kulmala, M., Ehn, M., and Sipilä, M.: Production of extremely low volatile organic compounds from biogenic emissions: Measured yields and atmospheric implications, Proceedings of the National Academy of Sciences, 112, 7123, 10.1073/pnas.1423977112, 2015a.

Jokinen, T., Berndt, T., Makkonen, R., Kerminen, V.-M., Junninen, H., Paasonen, P., Stratmann, F., Herrmann, H., Guenther, A. B., Worsnop, D. R., Kulmala, M., Ehn, M., and Sipilä, M.: Production of extremely low volatile organic compounds from biogenic emissions: Measured yields and atmospheric implications, Proceedings of the National Academy of Sciences, 112, 7123-7128, 10.1073/pnas.1423977112, 2015b.

Kenseth, C. M., Huang, Y., Zhao, R., Dalleska, N. F., Hethcox, J. C., Stoltz, B. M., and Seinfeld, J. H.: Synergistic O3 + OH oxidation pathway to extremely low-volatility dimers revealed in β-pinene secondary organic aerosol, Proceedings of the National Academy of Sciences, 201804671, 10.1073/pnas.1804671115, 2018.

Khaykin, S., Legras, B., Bucci, S., Sellitto, P., Isaksen, L., Tencé, F., Bekki, S., Bourassa, A., Rieger, L., Zawada, D., Jumelet, J., and Godin-Beekmann, S.: The 2019/20 Australian wildfires generated a persistent smoke-charged vortex rising up to 35 km altitude, Communications Earth & Environment, 1, 22, 10.1038/s43247-020-00022-5, 2020.

Kourtchev, I., Doussin, J. F., Giorio, C., Mahon, B., Wilson, E. M., Maurin, N., Pangui, E., Venables, D. S., Wenger, J. C., and Kalberer, M.: Molecular Composition of Fresh and Aged Secondary Organic Aerosol from a Mixture of Biogenic Volatile Compounds: A High-Resolution Mass Spectrometry Study, Atmos. Chem. Phys., 15, 5683, 2015.

Krechmer, J. E., Groessl, M., Zhang, X., Junninen, H., Massoli, P., Lambe, A. T., Kimmel, J. R., Cubison, M. J., Graf, S., Lin, Y. H., Budisulistiorini, S. H., Zhang, H., Surratt, J. D., Knochenmuss, R., Jayne, J. T., Worsnop, D. R., Jimenez, J. L., and Canagaratna, M. R.: Ion mobility spectrometry–mass

spectrometry (IMS–MS) for on- and offline analysis of atmospheric gas and aerosol species, Atmos. Meas. Tech., 9, 3245-3262, 10.5194/amt-9-3245-2016, 2016.
Kristensen, K., Watne, Å. K., Hammes, J., Lutz, A., Petäjä, T., Hallquist, M., Bilde, M., and Glasius, M.: High-Molecular Weight Dimer Esters Are Major Products in Aerosols from α-Pinene Ozonolysis and the Boreal Forest, Environmental Science & Technology Letters, 3, 280-285, 10.1021/acs.estlett.6b00152, 2016.
Kroll, J. H., Donahue, N. M., Jimenez, J. L., Kessler, S. H., Canagaratna, M. R., Wilson, K. R., Altieri, K. E., Mazzoleni, L. R., Wozniak, A. S., Bluhm, H., Mysak, E. R., Smith, J. D., Kolb, C. E., and Worsnop, D. R.: Carbon oxidation state as a metric for describing the chemistry of atmospheric organic aerosol, Nature Chemistry, 3, 133-139, 10.1038/nchem.948, 2011.
Kundu, S., Fisseha, R., Putman, A. L., Rahn, T. A., and Mazzoleni, L. R.: High molecular weight SOA formation during limonene ozonolysis: insights from ultrahigh-resolution FT-ICR mass spectrometry characterization, Atmos. Chem. Phys., 12, 5523-5536, 10.5194/acp-12-5523-2012, 2012.
Kurtén, T., Rissanen, M. P., Mackeprang, K., Thornton, J. A., Hyttinen, N., Jørgensen, S., Ehn, M., and Kjaergaard, H. G.: Computational Study of Hydrogen Shifts and Ring-Opening Mechanisms in α-Pinene Ozonolysis Products, The Journal of Physical Chemistry A, 119, 11366-11375, 10.1021/acs.jpca.5b08948, 2015.
Mazzoleni, L. R., Zielinska, B., and Moosmüller, H.: Emissions of Levoglucosan, Methoxy Phenols, and Organic Acids from Prescribed Burns, Laboratory Combustion of Wildland Fuels, and Residential Wood Combustion, Environmental Science & Technology, 41, 2115-2122, 10.1021/es061702c, 2007.
Melendez-Perez, J. J., Martínez-Mejia, M. J., and Eberlin, M. N.: A reformulated aromaticity index equation under consideration for non-aromatic and non-condensed aromatic cyclic carbonyl compounds, Organic Geochemistry, 95, 29-33, j.orggeochem.2016.02.002, 2016.
Meusinger, C., Dusek, U., King, S. M., Holzinger, R., Rosenørn, T., Sperlich, P., Julien, M., Remaud, G. S., Bilde, M., Röckmann, T., and Johnson, M. S.: Chemical and isotopic composition of secondary organic aerosol generated by α-pinene ozonolysis, Atmos. Chem. Phys., 17, 6373-6391, 10.5194/acp-17-6373-2017, 2017.
Nørgaard, A. W., Vibenholt, A., Benassi, M., Clausen, P. A., and Wolkoff, P.: Study of Ozone-Initiated Limonene Reaction Products by Low Temperature Plasma Ionization Mass Spectrometry, Journal of The American Society for Mass Spectrometry, 24, 1090-1096, 10.1007/s13361-013-0648-3, 2013.
Nozière, B., Kalberer, M., Claeys, M., Allan, J., D'Anna, B., Decesari, S., Finessi, E., Glasius, M., Grgić, I., Hamilton, J. F., Hoffmann, T., Iinuma, Y., Jaoui, M., Kahnt, A., Kampf, C. J., Kourtchev, I., Maenhaut, W., Marsden, N., Saarikoski, S., Schnelle-Kreis, J., Surratt, J. D., Szidat, S., Szmigielski, R., and Wisthaler, A.: The Molecular Identification of Organic Compounds in the Atmosphere: State of the Art and Challenges, Chemical Reviews, 115, 3919-3983, 10.1021/cr5003485, 2015.
Ohneiser, K., Ansmann, A., Baars, H., Seifert, P., Barja, B., Jimenez, C., Radenz, M., Teisseire, A., Floutsi, A., Haarig, M., Foth, A., Chudnovsky, A., Engelmann, R., Zamorano, F., Bühl, J., and Wandinger, U.: Smoke of extreme Australian bushfires observed in the stratosphere over Punta Arenas, Chile, in January 2020: optical thickness, lidar ratios, and depolarization ratios at 355 and 532 nm, Atmos. Chem. Phys., 20, 8003-8015, 10.5194/acp-20-8003-2020, 2020.
Oros, D. R., and Simoneit, B. R. T.: Identification and emission factors of molecular tracers in organic aerosols from biomass burning Part 1. Temperate climate conifers, Applied Geochemistry, 16, 1513-1544, 10.1016/S0883-2927(01)00021-X, 2001.
Otkjær, R. V., Jakobsen, H. H., Tram, C. M., and Kjaergaard, H. G.: Calculated Hydrogen Shift Rate Constants in Substituted Alkyl Peroxy Radicals, The Journal of Physical Chemistry A, 122, 8665-8673, 10.1021/acs.jpca.8b06223, 2018.
Pospisilova, V., Lopez-Hilfiker, F. D., Bell, D. M., El Haddad, I., Mohr, C., Huang, W., Heikkinen, L., Xiao, M., Dommen, J., Prevot, A. S. H., Baltensperger, U., and Slowik, J. G.: On the fate of oxygenated organic molecules in atmospheric aerosol particles, Science Advances, 6, eaax8922, 10.1126/sciadv.aax8922, 2020.

609 Quéléver, L. L. J., Kristensen, K., Normann Jensen, L., Rosati, B., Teiwes, R., Daellenbach, K. R.,
610 Peräkylä, O., Roldin, P., Bossi, R., Pedersen, H. B., Glasius, M., Bilde, M., and Ehn, M.: Effect of
611 temperature on the formation of highly oxygenated organic molecules (HOMs) from alpha-pinene
612 ozonolysis, Atmos. Chem. Phys., 19, 7609-7625, 10.5194/acp-19-7609-2019, 2019.
613 Savee, J. D., Papajak, E., Rotavera, B., Huang, H., Eskola, A. J., Welz, O., Sheps, L., Taatjes, C. A., Zádor,
614 J., and Osborn, D. L.: Carbon radicals. Direct observation and kinetics of a hydroperoxyalkyl radical
615 (QOOH), Science, 347, 643-646, 10.1126/science.aaa1495, 2015.
616 Shrivastava, M., Cappa, C. D., Fan, J. W., Goldstein, A. H., Guenther, A. B., Jimenez, J. L., Kuang, C.,
617 Laskin, A., Martin, S. T., Ng, N. L., Petaja, T., Pierce, J. R., Rasch, P. J., Roldin, P., Seinfeld, J. H.,
618 Shilling, J., Smith, J. N., Thornton, J. A., Volkamer, R., Wang, J., Worsnop, D. R., Zaveri, R. A.,
619 Zelenyuk, A., and Zhang, Q.: Recent advances in understanding secondary organic aerosol:
620 Implications for global climate forcing, Rev. Geophys., 55, 509, 2017.
621 Smith, J. S., Laskin, A., and Laskin, J.: Molecular Characterization of Biomass Burning Aerosols Using
622 High-Resolution Mass Spectrometry, Analytical Chemistry, 81, 1512-1521, 10.1021/ac8020664,
623 2009.
624 Tomaz, S., Wang, D., Zabalegui, N., Li, D., Lamkaddam, H., Bachmeier, F., Vogel, A., Monge, M. E.,
625 Perrier, S., Baltensperger, U., George, C., Rissanen, M., Ehn, M., El Haddad, I., and Riva, M.:
626 Structures and reactivity of peroxy radicals and dimeric products revealed by online tandem mass
627 spectrometry, Nature Communications, 12, 300, 10.1038/s41467-020-20532-2, 2021.
628 Tröstl, J., Chuang, W. K., Gordon, H., Heinritzi, M., Yan, C., Molteni, U., Ahlm, L., Frege, C., Bianchi, F.,
629 Wagner, R., Simon, M., Lehtipalo, K., Williamson, C., Craven, J. S., Duplissy, J., Adamov, A., Almeida,
630 J., Bernhammer, A.-K., Breitenlechner, M., Brilke, S., Dias, A., Ehrhart, S., Flagan, R. C., Franchin, A.,
631 Fuchs, C., Guida, R., Gysel, M., Hansel, A., Hoyle, C. R., Jokinen, T., Junninen, H., Kangasluoma, J.,
632 Keskinen, H., Kim, J., Krapf, M., Kürten, A., Laaksonen, A., Lawler, M., Leiminger, M., Mathot, S.,
633 Möhler, O., Nieminen, T., Onnela, A., Petäjä, T., Piel, F. M., Miettinen, P., Rissanen, M. P., Rondo, L.,
634 Sarnela, N., Schobesberger, S., Sengupta, K., Sipilä, M., Smith, J. N., Steiner, G., Tomè, A., Virtanen,
635 A., Wagner, A. C., Weingartner, E., Wimmer, D., Winkler, P. M., Ye, P., Carslaw, K. S., Curtius, J.,
636 Dommen, J., Kirkby, J., Kulmala, M., Riipinen, I., Worsnop, D. R., Donahue, N. M., and
637 Baltensperger, U.: The role of low-volatility organic compounds in initial particle growth in the
638 atmosphere, Nature, 533, 527-531, 10.1038/nature18271, 2016.
639 Van Krevelen, D. W.: Graphical-statistical method for the study of structure and reaction processes of
640 coal, Fuel, 29, 269-284, 1950.
641 Vereecken, L., Müller, J. F., and Peeters, J.: Low-volatility poly-oxygenates in the OH-initiated
642 atmospheric oxidation of α-pinene: impact of non-traditional peroxyl radical chemistry, Physical
643 Chemistry Chemical Physics, 9, 5241-5248, 10.1039/B708023A, 2007.
644 Vereecken, L., and Nozière, B.: H migration in peroxy radicals under atmospheric conditions, Atmos.
645 Chem. Phys., 20, 7429-7458, 10.5194/acp-20-7429-2020, 2020.
646 Walser, M. L., Desyaterik, Y., Laskin, J., Laskin, A., and Nizkorodov, S. A.: High-resolution mass
647 spectrometric analysis of secondary organic aerosol produced by ozonation of limonene, Physical
648 Chemistry Chemical Physics, 10, 1009-1022, 10.1039/B712620D, 2008.
649 Wang, Z., Ehn, M., Rissanen, M. P., Garmash, O., Quéléver, L., Xing, L., Monge-Palacios, M., Rantala,
650 P., Donahue, N. M., Berndt, T., and Sarathy, S. M.: Efficient alkane oxidation under combustion
651 engine and atmospheric conditions, Communications Chemistry, 4, 18, 10.1038/s42004-020-
652 00445-3, 2021a.
653 Wang, Z., Ehn, M., Rissanen, M. P., Garmash, O., Quéléver, L., Xing, L., Monge Palacios, M., Rantala,
654 P., Donahue, N. M., Berndt, T., and Sarathy, M.: - Efficient alkane oxidation under combustion
655 engine and atmospheric conditions, - Springer Science and Business Media LLC, 2021b.
656 Warscheid, B., and Hoffmann, T.: Structural elucidation of monoterpene oxidation products by ion
657 trap fragmentation using on-line atmospheric pressure chemical ionisation mass spectrometry in
658 the negative ion mode, Rapid Communications in Mass Spectrometry, 15, 2259-2272,
659 10.1002/rcm.504, 2001.

Witkowski, B., and Gierczak, T.: Characterization of the limonene oxidation products with liquid chromatography coupled to the tandem mass spectrometry, Atmospheric Environment, 154, 297-307, 10.1016/j.atmosenv.2017.02.005, 2017.

Xie, Q., Su, S., Chen, S., Xu, Y., Cao, D., Chen, J., Ren, L., Yue, S., Zhao, W., Sun, Y., Wang, Z., Tong, H., Su, H., Cheng, Y., Kawamura, K., Jiang, G., Liu, C. Q., and Fu, P.: Molecular characterization of firework-related urban aerosols using Fourier transform ion cyclotron resonance mass spectrometry, Atmos. Chem. Phys., 20, 6803-6820, 10.5194/acp-20-6803-2020, 2020.

Zhao, Y., Thornton, J. A., and Pye, H. O. T.: Quantitative constraints on autoxidation and dimer formation from direct probing of monoterpene-derived peroxy radical chemistry, Proc Natl Acad Sci U S A, 115, 12142-12147, 10.1073/pnas.1812147115, 2018.